The Canadian Mineralogist
Vol. 39, pp. 855-872 (2001)

MINERALOGY OF SULFOSALT-RICH VEIN-TYPE ORES, BOLIDEN MASSIVE SULFIDE DEPOSIT, SKELLEFTE DISTRICT, NORTHERN SWEDEN

THOMAS WAGNER[§]

Mineralogisches Institut der Universität Würzburg, Am Hubland, D-97074 Würzburg, Germany

ERIK JONSSON[§]

Department of Mineralogy, Swedish Museum of Natural History, Box 50007, SE-10405 Stockholm, Sweden

Abstract

Sulfosalt-rich vein-ores, which form an important mineralization type of the Paleoproterozoic metavolcanic-hosted Boliden Au–Cu–As massive sulfide deposit, in the Skellefte district, in northern Sweden, have been investigated by a combination of ore microscopy, electron-microprobe analysis and balanced reactions. The sample material contains a variety of ore minerals, including Au–Ag alloy, gudmundite, selenian galena, kobellite, tetrahedrite, bournonite and laitakarite. The vein ores display structures indicative of extensive deformation. Three distinct decomposition-induced assemblages, which postdate the deformation, have formed at the expense of kobellite: (i) selenian galena + laitakarite, (ii) tetrahedrite + laitakarite, and (iii) bournonite + laitakarite. Both kobellite and bournonite are unusually Se-rich, with concentrations in the range of 3.16–4.55 wt.% and 3.37–4.73 wt.%, respectively. Laitakarite, $Bi_4(Se,S)_3$, is characterized by substantial incorporation of Te, in the range of 0.94–9.64 wt.%. Comparable compositions have not been reported before and are indicative of extensive solid-solution within the system Bi_4S_3–Bi_4Se_3–Bi_4Te_3. Pb, with concentrations in the range of 3.01–4.56 wt.%, constitutes an essential component of laitakarite. The amount of Pb incorporation is approximately constant over the entire compositional range. Construction of balanced reactions for the principal types of decomposition textures demonstrates that these fluid-assisted replacement processes are controlled by individual pairs of immobile elements.

Keywords: sulfosalts, kobellite, laitakarite, Te incorporation, solid solution, decomposition reaction, Boliden, Skellefte district, Sweden.

Sommaire

Le minerai en veines riche en sulfosels, qui constitue un type de minéralisation important dans le gisement paléoprotérozoïque de Boliden (Au–Cu–As), dans le district de Skellefte, dans la partie nord de la Suède, dont l'hôte est métavolcanique, a été étudié par microscopie en lumière réfléchie, analyse à la microsonde électronique, et l'ébauche de réactions balancées. Le matériau étudié contient une variété de minéraux, dont un alliage Au–Ag, gudmundite, galène sélénifère, kobellite, tétraédrite, bournonite et laitakarite. Les textures dans le minerai en veines sont indicatives d'une déformation importante. Nous distinguons trois assemblages dus à une décomposition tardive de la kobellite: (i) galène sélénifère + laitakarite, (ii) tétraédrite + laitakarite, et (iii) bournonite + laitakarite. La kobellite et la bournonite possèdent des teneurs anormalement élevées en Se, de 3.16 à 4.55% et de 3.37 à 4.73% (poids), respectivement. La laitakarite, $Bi_4(Se,S)_3$, incorpore une quantité importante de Te, entre 0.94 et 9.64% (poids). Des compositions comparables n'avaient pas été signalées auparavant, et démontrent l'importance de solution solide dans le système Bi_4S_3–Bi_4Se_3–Bi_4Te_3. La concentration du Pb, dans l'intervalle 3.01–4.56%, montre que le plomb est ici un composant essentiel de la laitakarite. La teneur en Pb est à peu près constante sur l'intervalle de composition. L'ébauche de réactions balancées représentant les principaux types de textures de déstabilisation démontre que ces processus de remplacement en présence d'une phase fluide sont régis par des paires d'éléments immobiles.

(Traduit par la Rédaction)

Mots-clés: sulfosels, kobellite, laitakarite, incorporation de Te, solution solide, réaction de déstabilisation, Boliden, district de Skellefte, Suède.

§ *E-mail addresses*: thomas.wagner@mail.uni-wuerzburg.de, erik.jonsson@geo.su.se

INTRODUCTION

The Boliden Au–Cu–As massive sulfide deposit in the extensive Skellefte district, in Västerbotten County, northern Sweden, is well known for its high gold grades (average 15 ppm) and complex assemblages of ore minerals (*e.g.*, Ödman 1938, 1941, Grip & Wirstam 1970, Bergman Weihed *et al.* 1996). Two different types of mineralization constitute the Boliden deposit: (i) massive ore, composed of pyrite, arsenopyrite and minor pyrrhotite, and (ii) vein-type ores, composed of quartz, sulfides, tourmaline and sulfosalts, which cross-cut the massive orebodies and the country rocks (Grip & Wirstam 1970). Our recent investigation of brecciated arsenopyrite ore from dump material and glacial debris has revealed an unusual assemblage of Se-bearing sulfosalt minerals and Bi selenides of the laitakarite–ikunolite series in veins. We report the results of a systematic mineralogical and electron-microprobe study of these vein-type ores, complemented by modeling of the observed decomposition textures. The major objectives of this investigation are (1) to contribute to a characterization of the sulfosalt-rich vein ores, and (2) to place additional constraints on the late-stage evolution of the Boliden deposit.

BACKGROUND INFORMATION

The genetic evolution of the Boliden deposit has been the subject of extensive discussion. In contrast to earlier studies, which have placed the Boliden deposit among a class of syngenetic volcanic-exhalative massive sulfide deposits widespread in the Skellefte district (Rickard & Zweifel 1975, Vivallo 1987), recent structural, geochemical and Rb–Sr and U–Pb isotope investigations have indicated that it may be an example of a high-sulfidation epithermal style of mineralization (Bergman Weihed *et al.* 1996). The early geological and mineralogical studies focused on the vein-type ores, because of the associated economically important enrichments in gold, which locally reached maximum values in the range of 300–630 ppm (Mörtsell 1931, Ödman 1938, 1941). The vein-type ores can be subdivided into tourmaline–quartz veins, which mainly occur below the massive orebodies, and sulfide-hosted sulfosalt-rich veins (Grip & Wirstam 1970). Both types of vein assemblages are rich in various sulfosalts of Bi, Bi–Sb and Sb, including Se-bearing varieties of cosalite, kobellite and lillianite (Isaksson 1973). Besides Bi–Sb sulfosalt minerals and Fe–Co–Ni arsenides and antimonides, several Bi telluride phases (tetradymite, joséite-

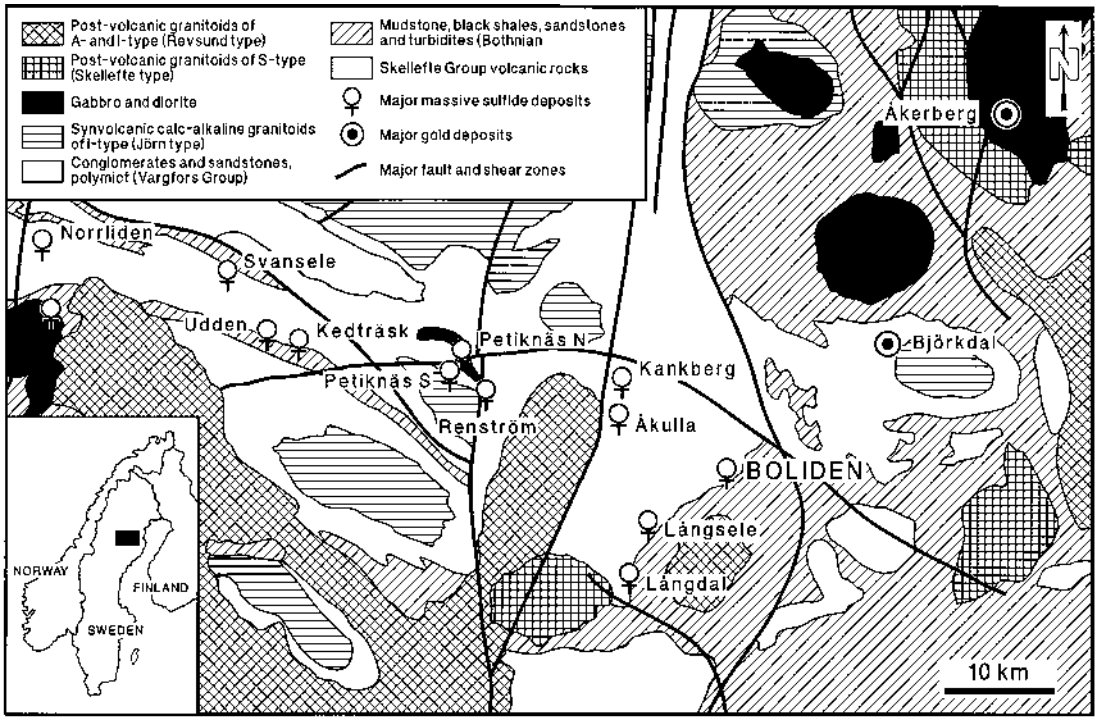

FIG. 1. Geological sketch-map of the central part of the Skellefte district, Sweden. Redrawn and modified after Bergman Weihed *et al.* (1996).

A, tellurobismutite) are present within arsenopyrite ore and quartz–tourmaline veins (Grip & Wirstam 1970, Isaksson 1973).

Geological Setting and Sample Location

The Paleoproterozoic Skellefte district covers an area of about 150 × 40 km within the northern part of the *ca.* 1.8–2.0 Ga Svecofennian Subprovince (Fig. 1). The Skellefte district forms a relatively distinct belt of mainly submarine metavolcanic-rock-hosted sulfide ore deposits; it is elongate approximately in an east–west direction (Rickard 1986, Weihed *et al.* 1992). The metavolcanic and metasedimentary host-rocks to the ore were formed *ca.* 1.89–1.85 Ga ago (Billström & Weihed 1996) in a volcanic arc setting; they comprise a succession of submarine volcanic and subvolcanic rocks and clastic sedimentary units (Allen *et al.* 1996). Peak regional Svecokarelian metamorphism of greenschist to amphibolite grade affected the area at *ca.* 1.83–1.81 Ga (Billström & Weihed 1996). The massive sulfide deposits of the Skellefte district commonly occur close to the interface between the upper metavolcanic rocks (mainly rhyolite to dacite) of the Skellefte Group and the overlying metasedimentary units (graywackes and mudstones with intercalated mafic metavolcanic rocks) of the Vargfors Group (Bergman Weihed *et al.* 1996).

The metavolcanic unit hosting the Boliden ores is considered to represent the metamorphosed equivalent of a subaqueous to partially subaerial rhyolitic cryptodome-tuff volcano. Although the previously held view was that the ores represented metamorphosed equivalents of Kuroko-type ores, it was recently suggested by Allen *et al.* (1996) that the major part of massive sulfide mineralization in the Skellefte district formed as high-sulfidation-type epithermal sub-seafloor infiltrations and replacements. The massive sulfide ores at Boliden occur as an elongate set of lenses, obliquely cutting the host rocks in a structure approximately oriented east–west with a roughly vertical dip. The orientation of the ore zones has been related to a local shear zone (Bergman Weihed *et al.* 1996) responsible for the tectonic deformation evident in sulfides and sulfosalts. Ore formation started with the massive sulfide ores (pyrite and arsenopyrite ores) and the coeval alteration of the host rocks, with an inner zone dominated by white mica ± andalusite, and an outer chlorite-dominated zone (Ödman 1941, Bergman Weihed *et al.* 1996). Later, localized deformation caused the stretching and detachment of the bodies of massive ore, as well as subsequent formation of the gold-bearing sulfosalt – quartz – sulfide veins. The vein assemblages were tectonized at an even later stage, as is indicated by the omnipresent deformation textures in the sulfosalts and sulfides; the recrystallization of arsenopyrite postdates the deformation of the veins. Bergman Weihed *et al.* (1996) suggested that the initial vein-forming (brecciation) event took place around 1.85–1.82 Ga, and prior to the *ca.* 1.83–1.81 Ga peak Svecokarelian metamorphism; they further suggested that the abundant recrystallization of sulfides took place during peak metamorphic conditions.

Samples of the sulfosalt-bearing arsenopyrite-hosted vein-type ore were collected in mine dumps at Boliden. The mine, closed since 1967, is now water-filled and inaccessible. Investigations have to rely on material from old collections, drill cores and material collected on the remaining dumps. The ore-bearing boulders sampled at the dump date from the early stages of mining the Boliden deposit; several of them are glacially rounded and associated with sandy glacial till. The Boliden deposit was covered with a blanket of glacial debris up to 19 m thick (Ödman 1941), and large amounts of this had to be excavated, together with loose boulders of ore and host rocks, before mining could commence in the superficial orebodies. The samples investigated correspond to sulfosalt–quartz-veined arsenopyrite ore of the type mined in the uppermost parts of the orebody at Boliden. They are characterized by an abundance of millimetric to centimetric veins of megascopically visible sulfosalts, quartz and sulfides occurring in a brecciated, very fine-grained arsenopyrite-dominated massive ore.

Textural Relationships of the Vein-Type Ores

The vein-type mineralization investigated here occurs as networks of numerous veinlets, 20 μm to over 10 mm in width, within intensely brecciated portions of massive arsenopyrite ore. Besides quartz, calcite and rutile, which are the most common gangue minerals, these veinlets contain a large number of ore minerals, including a gold–silver alloy, native bismuth, pyrite, pyrrhotite, sphalerite, chalcopyrite, cubanite, gudmundite, galena, kobellite, tetrahedrite, bournonite and laitakarite. Most vein assemblages have been extensively deformed and display ductile shearing, the *durchbewegung* structure (see definition in Marshall & Gilligan 1989), or brecciation, depending on the competence (or competence contrast) of the respective minerals. Rutile, which forms idiomorphic blocky crystals within narrow veinlets in massive arsenopyrite, was brecciated, and displays infilling by chalcopyrite, pyrrhotite and kobellite (Fig. 2a). Irregularly shaped grains of Au–Ag alloy, 2–50 μm in size, are exclusively found in very narrow veinlets closely associated with bournonite, kobellite and chalcopyrite, and have preferentially formed along the vein contacts with arsenopyrite (Fig. 2b). Most of the wider veinlets in massive arsenopyrite, which are completely filled by kobellite, were subjected to ductile shearing. This mineral shows a foliated texture, composed of elongate subparallel grains of kobellite with numerous inclusions of lath-shaped and anhedral elongate grains of laitakarite, 5–90 μm long and 1–10 μm wide, which are oriented parallel to the foliation. Minor localized shear zones hosting complex assemblages composed of kobellite, chalcopyrite,

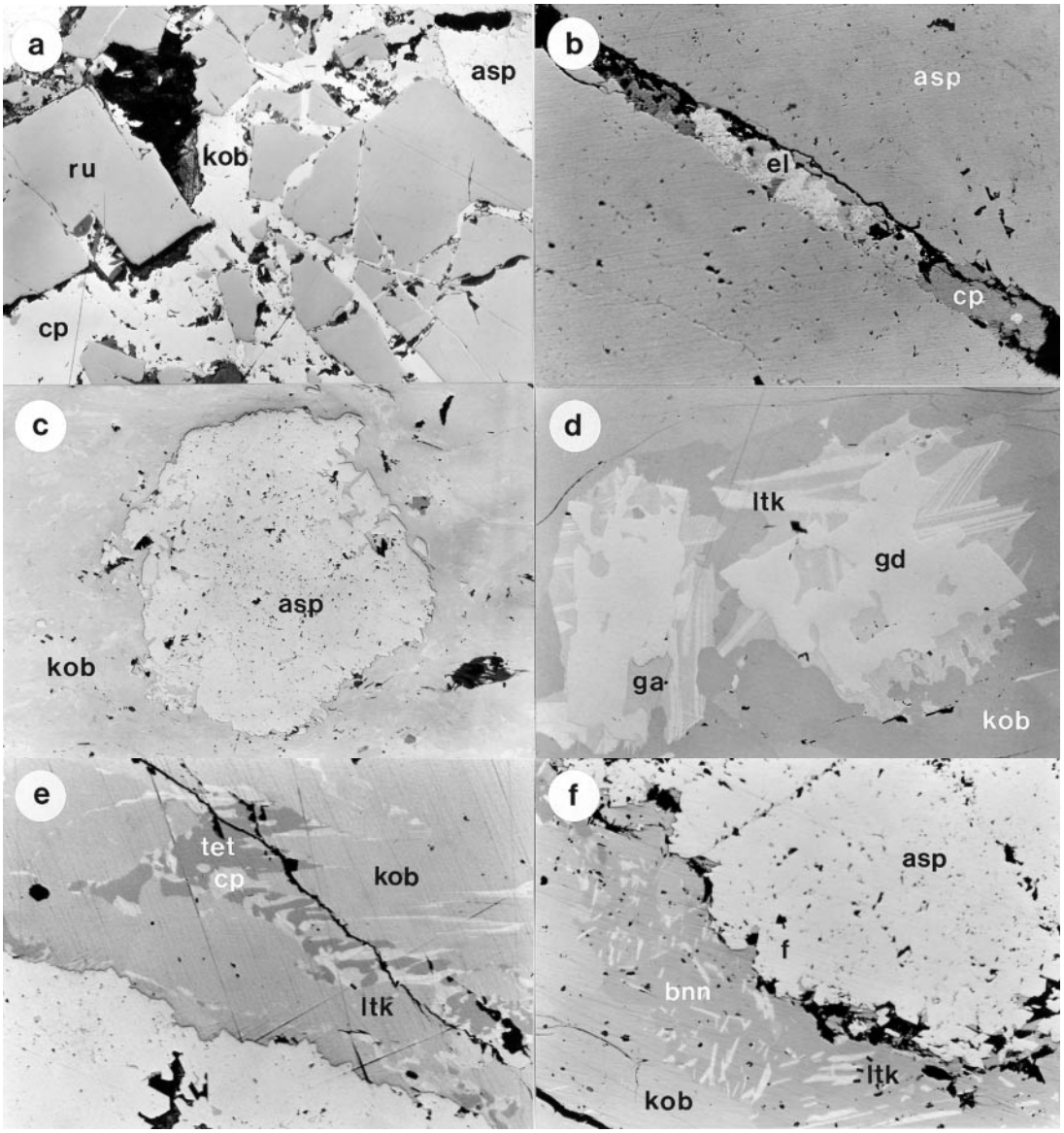

FIG. 2. Photomicrographs in reflected light showing representative textural relationships of sulfosalt-rich vein-type ores, Boliden deposit. (a) Idiomorphic blocky crystals of rutile (ru) within a veinlet in massive arsenopyrite (asp). After brecciation of the rutile, chalcopyrite (cp) and kobellite (kob) both infilled microfractures. Sample EJ–B4. Width of field: 1.43 mm. (b) Anhedral grains of "electrum" (el) in close association with chalcopyrite (cp) in a narrow veinlet in massive arsenopyrite (asp). Sample EJ–B4. Width of field: 240 μm. (c) *Durchbewegung* structure. A single rotated fractured clast of arsenopyrite (asp) is enclosed within kobellite (kob), which was subjected to ductile deformation. Pressure shadows of the arsenopyrite clast display extensive recrystallization. Sample EJ–B3a. Width of field: 860 μm. (d) Typical occurrence of gudmundite (gd) inclusions within kobellite (kob). Gudmundite is commonly surrounded by a decomposition texture composed of lath-shaped laitakarite (ltk) crystals and anhedral selenian galena (ga). Sample EJ–B6a. Width of field: 310 μm. (e) Complex decomposition-induced symplectitic texture composed of tetrahedrite (tet) and laitakarite (ltk), which have formed at the expense of kobellite (kob). Relict inclusions of chalcopyrite (cp) display extensive corrosion. Sample EJ–B8. Width of field: 360 μm. (f) Decomposition texture within kobellite (kob), composed of bournonite (bnn) and laitakarite (ltk), which have preferentially formed along the grain boundaries between kobellite and arsenopyrite (asp). Sample EJ–B3b. Width of field: 450 μm.

pyrrhotite, arsenopyrite and gangue minerals are characterized by the *durchbewegung* structure, resulting from heterogeneous flow due to significant contrasts in the competence of the deformed sulfide and gangue minerals (Marshall & Gilligan 1989). As a consequence, rotated fractured clasts of arsenopyrite and quartz are commonly hosted in a matrix of chalcopyrite, pyrrhotite and kobellite, which indicates ductile deformation. Pressure shadows of the arsenopyrite clasts commonly display extensive recrystallization (Fig. 2c). Several of the veinlets are filled by deformed pyrrhotite and chalcopyrite, which display banded textures and elongate grain-shapes. The chalcopyrite generally contains inclusions of idiomorphic pyrite, whereas pyrrhotite is rarely intergrown with coarse-grained cubanite. In addition to the common association between kobellite and chalcopyrite–pyrrhotite assemblages, kobellite rarely hosts inclusions of tetrahedrite and gudmundite as well as very minute (<1 to 3 μm) irregularly shaped grains of native bismuth. Coarse-grained anhedral aggregates of sphalerite have preferentially overgrown and enclosed chalcopyrite, which is commonly present as corroded relict grains within sphalerite. In addition, sphalerite is also intimately intergrown with complex assemblages composed of chalcopyrite, pyrrhotite and sulfosalts.

The decomposition of kobellite

The most characteristic feature of the sulfosalt-rich samples is the omnipresence of various decomposition textures, which clearly postdate the deformation of the vein-type ores. The decomposition of kobellite has preferentially occurred along the grain boundaries between kobellite and arsenopyrite, close to microfractures and around inclusions of gudmundite within kobellite. Three distinct decomposition-induced assemblages have been identified: (i) selenian galena + laitakarite, (ii) tetrahedrite + laitakarite, and (iii) bournonite + laitakarite. Kobellite enclosing subhedral to euhedral grains of gudmundite very commonly displays a characteristic reaction rim composed of lath-shaped crystals of laitakarite and anhedral grains of selenian galena. The laitakarite crystals are arranged in subparallel groups and are dominantly oriented perpendicular to the former grain-boundaries between kobellite and gudmundite (Fig. 2d). The symplectitic association tetrahedrite + laitakarite seems to be related to chalcopyrite inclusions in kobellite (Fig. 2e). Chalcopyrite occurs as heavily corroded relict grains within the symplectitic tetrahedrite–laitakarite assemblage. Finally, kobellite has very commonly decomposed to a complex rim composed of bournonite and clusters of lath-shaped to acicular crystals of laitakarite (Fig. 2f). The formation of this association is restricted to grain boundaries between kobellite and arsenopyrite, thereby indicating that this decomposition reaction was fluid-assisted.

COMPOSITIONAL DATA

Analytical method

The chemical composition of mineral phases was determined by wavelength-dispersion electron-probe microanalysis using the CAMECA SX–50 instrument in Würzburg. Operating conditions were 15 kV at a beam current of 15 nA, a beam size of 1–2 μm and counting times of 20 s on TAP/PET and 30 s on LIF crystals. Standards and radiation used were as follows: Se*L*α, Te*L*α, Cd*L*α, Ag*L*α, Bi*M*α, Au*M*α, Cu*K*α, Co*K*α and Ni*K*α, GaAs (As*L*α), FeS_2 (Fe*K*α, S*K*α), ZnS (Zn*K*α), Sb_2S_3 (Sb*L*α), PbS (Pb*M*α), HgS (Hg*M*α), SnO_2 (Sb*L*α) and $MnTiO_3$ (Mn*K*α). Under the current operating conditions, the analytical precision is approximately 1% for all major elements; the detection limit is around 0.1 wt.%.

Native elements

The precious metal alloy, detected only in two of the samples investigated, displays extensive compositional variability, even at the local scale. It contains essentially Au, Ag and Hg, whereas all other elements sought are, with the exception of minor concentrations of Cu, below the detection limit. The compositional limits vary between $Au_{0.63}Ag_{0.37}$ and $Au_{0.37}Ag_{0.57}Hg_{0.06}$. The compositions correspond well with analytical data reported for Au-bearing alloy from quartz veinlets in arsenopyrite ore and from brecciated arsenopyrite ore associated with Bi–Se mineralization (Bergman Weihed *et al.* 1996). The native bismuth, present as inclusions within kobellite, is close to being pure; only minor concentrations of Sb in the range of 0.5–2.0 wt.% were detected.

Sulfides

Chalcopyrite, cubanite, and pyrite have compositions close to stoichiometry, whereas pyrrhotite displays a narrow compositional range between $Fe_{0.84}S_{1.00}$ and $Fe_{0.86}S_{1.00}$. The levels of concentration of trace elements in all Fe–(Cu) sulfides, notably of Co and Ni, are generally below 0.1 wt.%. Sphalerite carries significant levels of Fe and Cd, in the range of 6.15–7.48 wt.% and 0.51–0.85 wt.%, respectively. The frequency distributions of both elements indicate a rather homogeneous composition of sphalerite from all samples investigated, independent of the respective textural association. The concentrations of Cu and Mn are relatively low, usually in the range of 0.1–0.2 wt.%. Gudmundite, exclusively found as inclusions within kobellite, shows low but detectable Se and Te contents, which attain 0.32 wt.% ($\bar{x}$ = 0.15; n = 11) and 0.49 wt.% ($\bar{x}$ = 0.20; n = 11). The level of incorporation of Co and Ni into gudmundite is insignificant; the concentrations of both elements are

generally below 0.1 wt.%. Selenian galena displays a very limited range of solid solution, between (Pb,Bi,Ag)$_{0.99}$S$_{0.67}$Se$_{0.33}$ and (Pb,Bi,Ag)$_{1.01}$S$_{0.66}$Se$_{0.35}$, whereas substitution of Pb by Bi and Ag is significant and varies considerably (Table 1). Bi, in the range 0.68–2.89 wt.%, exceeds the amount of Ag, between 0.14 and 0.98 wt.%. These data indicate that Bi is not entirely bound in a galena–matildite solid-solution (*e.g.*, Foord & Shawe 1989), but part of the Bi is incorporated according to the substitution scheme $3\,Pb^{2+} = 2\,Bi^{3+} + \square$ (Makovicky 1977).

Kobellite

This most abundant Pb–Sb–Bi sulfosalt mineral of the vein-type ores displays a relatively limited compositional variability (Table 2). The Bi/(Bi + Sb) atomic ratio calculated on the basis of 62 analyses ranges between 0.36 and 0.43, with a mean value of 0.39 (σ = 0.01). The observed composition of kobellite from the Boliden vein ores lies within the compositional range of kobellite and tintinaite (the Sb end-member) reported from other localities (Harris *et al.* 1968, Moëlo *et al.* 1984, 1995, Makovicky & Mumme 1986, Zakrzewski & Makovicky 1986). The general crystal-chemical formula for the kobellite homologous series results in (Cu,Fe)$_2$(Pb,Bi,Sb)$_{26}$(S,Se)$_{35}$ for both kobellite and tintinaite (Zakrzewski & Makovicky 1986, Makovicky 1989). Taking into consideration that the unit cell of kobellite contains two formula units (Makovicky & Mumme 1986), results of all microprobe analyses were recalculated on the basis of 52 octahedrally coordinated cations, including Pb, Sb, Bi and Ag. On the basis of

TABLE 1 REPRESENTATIVE RESULTS OF ELECTRON-MICROPROBE ANALYSES OF SELENIAN GALENA, BOLIDEN MASSIVE SULFIDE DEPOSIT

Sample	EJ-B6a 24	EJ-B6a 30	EJ-B6a 36	EJ-B6c 31	EJ-B6c 36	EJ-B6c 37
Cu wt %	<0.1	<0.1	<0.1	<0.1	0.11	<0.1
Ag	0.98	0.33	0.35	0.23	0.14	0.30
Fe	0.19	0.12	<0.1	<0.1	0.21	<0.1
Pb	76.77	77.34	79.58	79.09	80.04	78.83
Sb	0.13	<0.1	<0.1	<0.1	<0.1	0.11
Bi	2.47	2.89	1.07	2.09	0.68	1.31
S	8.41	8.21	8.46	8.41	8.44	8.30
Se	10.96	10.63	10.41	10.82	10.56	10.63
Te	0.11	0.15	<0.1	<0.1	<0.1	<0.1
total	100.02	99.67	99.87	100.64	100.18	99.48
	Formulae (Σ cations = 1)					
Ag	0.02	0.01	0.01	0.01	0.00	0.01
Pb	0.93	0.94	0.97	0.97	0.97	0.97
Bi	0.03	0.03	0.01	0.03	0.01	0.02
S	0.66	0.65	0.67	0.66	0.66	0.66
Se	0.35	0.34	0.33	0.35	0.34	0.34

TABLE 2. REPRESENTATIVE RESULTS OF ELECTRON-MICROPROBE ANALYSES OF KOBELLITE, BOLIDEN MASSIVE SULFIDE DEPOSIT

	EJ-B1 17	EJ-B2 24	EJ-B2 27	EJ-B3b 10	EJ-B4 28	EJ-B6a 12	EJ-B6a 14	EJ-B6a 47	EJ-B7a 44	EJ-B8 28
Cu wt.%	1.22	1.15	1.11	1.28	1.14	1.00	1.08	1.06	1.25	1.35
Ag	0.62	0.41	0.42	0.33	0.55	0.51	0.46	0.54	0.48	0.42
Fe	0.73	0.87	0.92	0.75	1.16	0.85	0.73	0.93	0.83	0.73
Pb	36.48	37.83	37.10	36.66	36.48	37.58	37.54	36.86	36.33	36.46
Sb	19.37	18.73	18.82	18.21	18.45	19.54	18.77	17.07	18.85	19.19
Bi	19.64	20.36	20.05	20.98	20.03	19.15	20.08	22.00	19.44	20.97
S	16.95	17.29	17.30	17.22	16.55	17.07	17.04	17.00	16.78	16.88
Se	4.38	4.07	4.11	3.81	4.23	4.10	4.01	3.16	4.55	4.21
total	99.39	100.71	99.83	99.24	98.59	99.80	99.71	98.62	98.51	100.21
	Formulae (calculated to 52 octahedrally coordinated cations)									
Cu	2.29	2.14	2.09	2.44	2.18	1.87	2.03	2.02	2.39	2.52
Ag	0.69	0.45	0.46	0.37	0.62	0.56	0.51	0.61	0.54	0.46
Fe	1.57	1.86	1.97	1.62	2.52	1.81	1.56	2.02	1.80	1.56
Pb	21.05	21.69	21.48	21.40	21.36	21.53	21.63	21.60	21.32	20.90
Sb	19.02	18.28	18.54	18.09	18.39	19.04	18.40	17.01	18.83	18.72
Bi	11.24	11.58	11.51	12.14	11.63	10.87	11.47	12.78	11.31	11.92
S	63.21	64.08	64.72	64.95	62.65	63.17	63.42	64.34	63.65	62.53
Se	6.63	6.12	6.25	5.84	6.51	6.17	6.05	4.86	7.01	6.33
$^{[6]}$Ag										
N(T$^+$)	2.33	2.36	2.33	2.29	2.36	2.36	2.36	2.39	2.32	2.24
N(T^{2+})	1.79	1.81	1.78	1.75	1.81	1.81	1.81	1.84	1.78	1.71
$^{[4]}$Ag										
N(T$^+$)	2.17	2.25	2.22	2.20	2.21	2.23	2.24	2.24	2.20	2.14
N(T^{2+})	1.66	1.72	1.70	1.68	1.69	1.71	1.72	1.72	1.68	1.63

these calculations and the assumption that Ag is entirely incorporated into such sites, the occupancy of the tetrahedrally coordinated metal sites by (Cu + Fe) ranges between 3.59 and 4.70 atoms per formula unit, *apfu* ($\bar{x}$ = 4.05; σ = 0.21), which is close to the ideal value of 4 *apfu*. A comparison of the variability of Cu and Fe atoms on tetrahedral sites with reported data on kobellite compositions in the literature cited indicates that incorporation of Fe in the tetrahedral sites is limited to approximately 2 *apfu* (Fig. 3). No composition of kobellite or tintinaite close to the crystal-chemically possible Fe-rich end-member has been reported to date (Moëlo *et al.* 1995). The incorporation of substantial Ag, in the range of 0.37–0.69 *apfu*, close to the amount of Ag reported for kobellite from other occurrences, constitutes a characteristic crystal-chemical feature of sulfosalt phases in the kobellite homologous series (Makovicky & Mumme 1986, Zakrzewski & Makovicky 1986, Cook 1997).

Calculation of the order of homologue (N) for the kobellite compositions from the Boliden vein ores has been carried out following the suggestions by Zakrzewski & Makovicky (1986). The values of N were calculated alternatively for Ag substituting completely on either octahedral or tetrahedral sites. For both cases, the resulting values of N are in the range 1.71–2.39 (Ag on octahedral sites) and 1.63–2.25 (Ag on tetrahedral sites). A characteristic compositional feature of kobellite from the vein-type ores investigated is a significant incorporation of Se, in the range of 3.16–4.55 wt.% ($\bar{x}$ = 4.01 wt.%; σ = 0.24 wt.%), corresponding to 4.86–7.01 *apfu*. The concentrations of Se are comparable to analytical data reported for kobellite from quartz veinlets in arsenopyrite ore and quartz–tourmaline veins of the Boliden deposit (Moëlo *et al.* 1984). In contrast to the high level of Se substitution, Te concentrations are very low and generally below 0.1 wt.%.

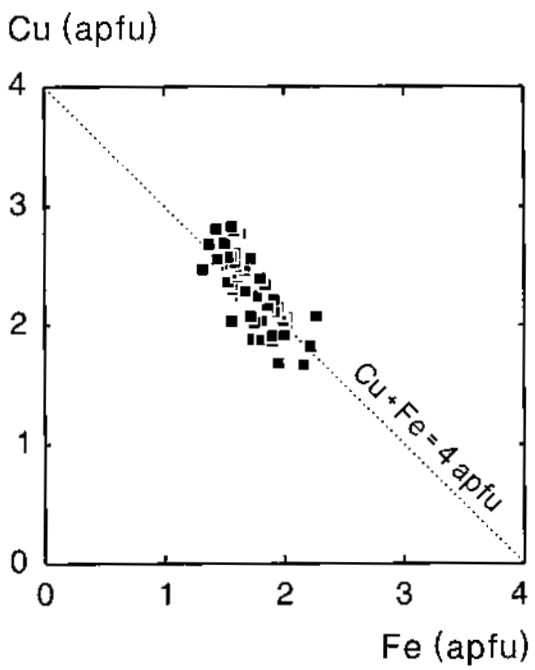

FIG. 3. Variation of Cu and Fe contents (expressed in *apfu*) in kobellite. The occupancy of the tetrahedral sites is generally very close to the ideal value, (Cu + Fe) = 4 *apfu*. The shaded area displays the range of kobellite compositions reported in the literature (see text for references).

Tetrahedrite

On the basis of textural association and composition, two distinct types of tetrahedrite can be distinguished (Fig. 4). Type 1, present as irregularly shaped inclusions

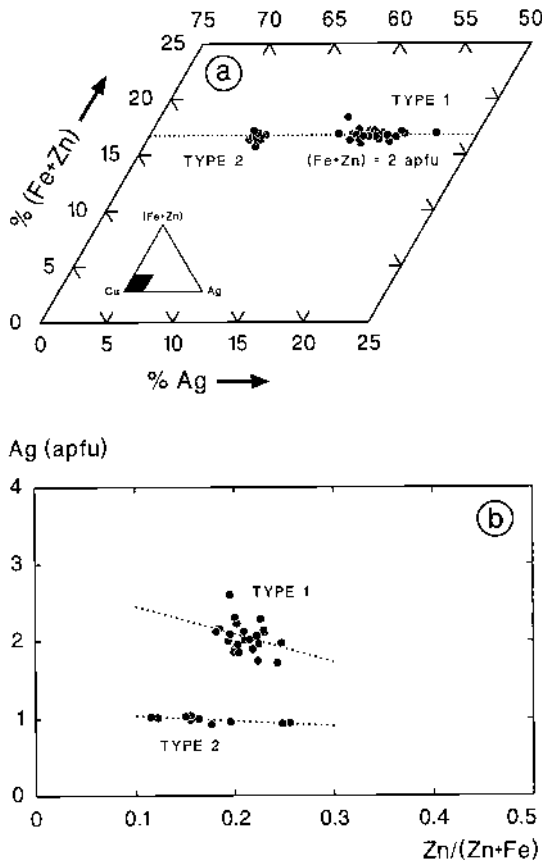

FIG. 4. Compositional variation of tetrahedrite from sulfosalt-rich vein ores. Tetrahedrite of type 1 is generally Ag-rich and shows variable Ag contents, whereas type-2 tetrahedrite displays a relatively constant Ag content. (a) Diagram Cu–Ag–(Fe + Zn), (b) Plot of Ag (*apfu*) *versus* Zn/(Zn + Fe).

TABLE 3. REPRESENTATIVE RESULTS OF ELECTRON-MICROPROBE ANALYSES OF TETRAHEDRITE, BOLIDEN MASSIVE SULFIDE DEPOSIT

	EJ-B7a 42	EJ-B7a 52	EJ-B7a 56	EJ-B7b 3	EJ-B7b 6	EJ-B7b 9	EJ-B3b 8	EJ-B8 11	EJ-B8 17	EJ-B8 18
Cu wt.%	28.22	29.51	29.93	28.70	28.09	26.08	33.55	33.53	32.50	32.81
Ag	13.28	10.59	10.86	12.78	13.65	15.77	6.05	5.86	6.50	6.43
Fe	5.17	5.02	5.00	4.96	4.88	5.08	4.81	5.49	5.47	5.73
Zn	1.36	1.89	1.68	1.65	1.45	1.44	1.93	1.38	1.18	0.87
Sb	27.88	28.12	28.34	27.93	27.95	27.85	29.74	28.80	28.66	28.82
Bi	<0.1	0.20	0.24	0.12	0.18	<0.1	0.16	0.23	0.29	0.25
S	23.80	23.69	23.67	23.85	23.78	23.60	24.66	24.39	24.15	24.43
Se	0.21	0.17	0.30	0.26	0.14	0.23	<0.1	0.12	0.12	0.19
total	99.92	99.19	100.02	100.25	100.12	100.05	100.90	99.80	98.87	99.53
	Formulae (Σ cations = 16)									
Cu	7.80	8.13	8.17	7.89	7.78	7.31	8.94	8.99	8.84	8.87
Ag	2.16	1.72	1.75	2.07	2.23	2.60	0.95	0.93	1.04	1.02
Fe	1.63	1.57	1.55	1.55	1.54	1.62	1.46	1.68	1.69	1.76
Zn	0.37	0.51	0.45	0.44	0.39	0.39	0.50	0.36	0.31	0.23
Sb	4.02	4.04	4.04	4.01	4.04	4.07	4.14	4.03	4.07	4.07
S	13.04	12.93	12.81	12.99	13.05	13.10	13.02	12.96	13.02	13.09
Se	0.05	0.04	0.07	0.06	0.03	0.05	0	0.03	0.03	0.04

Columns 1–6 contain compositions of type 1, whereas columns 7–10 contain compositions of type 2.

TABLE 4. REPRESENTATIVE RESULTS OF ELECTRON-MICROPROBE ANALYSES OF BOURNONITE, BOLIDEN MASSIVE SULFIDE DEPOSIT

Sample	EJ-B1 12	EJ-B3b 1	EJ-B3b 6	EJ-B7a 41	EJ-B1 7	EJ-B1 8
Cu wt.%	12.60	12.54	13.05	12.85	12.91	12.95
Pb	41.71	40.47	40.08	41.21	42.38	41.58
Sb	23.95	23.59	23.55	23.81	25.61	25.45
Bi	1.56	1.77	1.97	1.53	0.45	0.41
S	18.10	17.41	17.39	17.56	19.14	18.66
Se	3.37	4.17	4.51	4.73	1.15	2.01
total	101.29	99.95	100.55	101.69	101.64	101.06
	Formulae (Σ cations = 3)					
Cu	0.98	0.99	1.02	1.00	0.98	0.99
Pb	0.99	0.98	0.96	0.98	0.98	0.98
Sb	0.97	0.97	0.96	0.97	1.01	1.02
Bi	0.04	0.04	0.05	0.04	0.01	0.01
S	2.79	2.72	2.70	2.71	2.87	2.84
Se	0.21	0.27	0.28	0.30	0.07	0.12

within kobellite, is Ag-rich, with Ag concentrations in the range between 1.72 and 2.60 *apfu* (based on 16 cations). The Ag concentrations are only weakly correlated with the Zn/(Zn + Fe) atomic ratio ($R^2 = 0.11$), which vary within the range 0.19–0.24. In contrast, tetrahedrite of type 2, which is present as symplectitic intergrowths with laitakarite, displays a rather homogeneous concentration of Ag, approximately 0.93–1.04 *apfu*, whereas the Zn/(Zn + Fe) atomic ratio varies between 0.11 and 0.26 (Fig. 4b); the concentration of Ag is fairly well correlated with the Zn/(Zn + Fe) ratio ($R^2 = 0.55$). The occupancy of tetrahedral (Fe + Zn) positions is very close to the ideal value of 2 *apfu* for both types (Fig. 4a, Table 3). Most analyzed grains contain low but detectable concentrations of Bi and Se.

Bournonite

Bournonite displays a significant incorporation of Se, in the range of 1.15–4.73 wt.%, corresponding to 0.07–0.30 *apfu*, whereas Te concentrations are generally below 0.1 wt.% (Table 4). Bournonite present as a decomposition product of Se-rich kobellite is characterized by a range of Se concentrations (3.37–4.73 wt.%), very close to that of the precursor kobellite. In contrast, coarse-grained bournonite, which has not formed at the expense of kobellite, shows lower levels of Se, in the range 1.15–2.01 wt.%. In addition to Se, bournonite carries significant concentrations of Bi, in the range 0.41–1.97 wt.%.

Laitakarite, $Bi_4(Se,S)_3$

In the sulfosalt-rich vein ores, laitakarite is characterized by a significant compositional variability. Most of the grains display substantial incorporation of Te, in the range 1.05–9.64 wt.%, corresponding to 0.08–0.73 *apfu*, on the basis of a recalculation of the analytical data to (S + Se + Te) = 3 *apfu* (Figs. 5, 6). Two distinct populations can be distinguished on the basis of the textural relationships and composition. Laitakarite present as inclusions within kobellite displays a relatively high level of Te incorporation, in the range of 5.78–9.64 wt.%

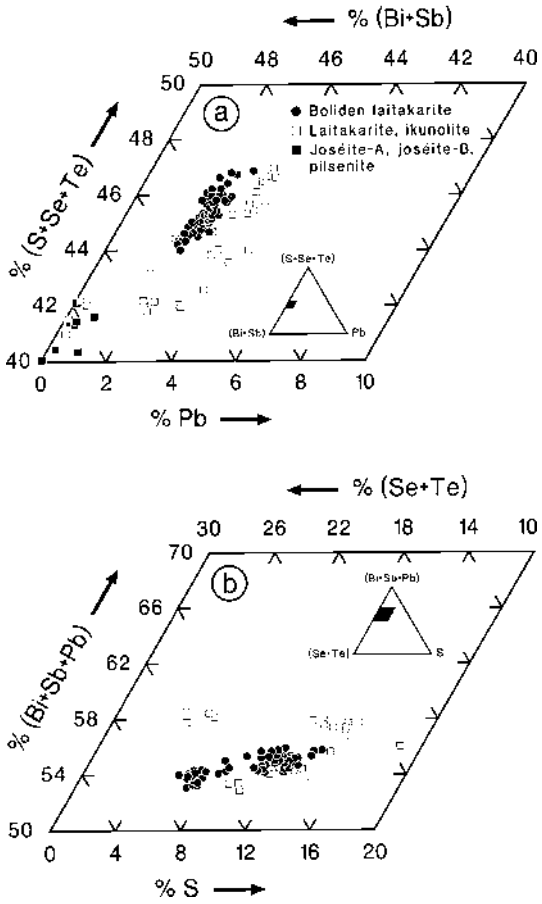

(Table 5), whereas laitakarite formed as a decomposition product of kobellite has lower concentrations of Te, in the range 1.05–4.08 wt.% (Table 6). The concentration of Se in laitakarite in the Boliden samples is generally very close to 2 *apfu*, which is in agreement with most analytical data reported for laitakarite from other occurrences (*e.g.,* Karup-Møller 1970, Zavyalov *et al.* 1983, Nenasheva *et al.* 1988, Yefimov *et al.* 1988).

A significant compositional characteristic of laitakarite from the Boliden vein ores is the presence of a substantial concentration of Pb, in the range 3.01–4.56 wt.%, corresponding to 0.14–0.21 *apfu* (Tables 5, 6). The Pb concentration is approximately constant over the entire compositional range, which is clearly seen in the Pb – (Bi + Sb) – (S + Se + Te) diagram (Fig. 5a). If the proportions of Bi, Se, S and Pb *apfu* are plotted as a function of increasing degree of Te content (Fig. 7), one sees that Te is negatively correlated with S ($R^2 = 0.85$), Se ($R^2 = 0.53$) and Bi ($R^2 = 0.67$), whereas the concentration of Pb seems to be independent of the level of Te ($R^2 = 0$) over the entire compositional range. All analytical data for laitakarite from the Boliden vein ores display a significant deficiency in cations, when normalized to (S + Se + Te) = 3 *apfu*. The calculated *Me*:(S + Se + Te) values are in the range between 3.41:3 and 3.78:3. Interestingly, the nonstoichiometry is largest for the most Te-rich compositions at Boliden.

FIG. 5. Compositional representations of laitakarite from sulfosalt-rich vein ores in terms of (a) the system Pb – (Bi + Sb) – (S + Se + Te), and (b), the system (Bi + Sb + Pb) – (Se + Te) – S. Analytical data on $Bi_4(S,Se,Te)_3$ phases reported in the literature are given for comparison (see text for references).

TABLE 5. REPRESENTATIVE RESULTS OF ELECTRON-MICROPROBE ANALYSES OF Te-RICH LAITAKARITE PRESENT AS INCLUSIONS IN KOBELLITE, BOLIDEN MASSIVE SULFIDE DEPOSIT

	EJ-B3a 14	EJ-B3a 16	EJ-B8 46	EJ-B8 47	EJ-B8 51	EJ-B8 53	EJ-B8 58	EJ-B8 60	EJ-B8 62	EJ-B8 64
Cu wt.%	<0.1	<0.1	<0.1	0.11	<0.1	<0.1	<0.1	<0.1	0.11	0.11
Pb	4.06	3.66	3.09	3.54	3.01	3.16	4.56	4.12	4.27	3.60
Sb	0.52	0.44	0.46	0.50	0.50	0.56	0.41	0.42	0.23	0.52
Bi	70.80	70.96	70.49	71.04	72.04	71.97	69.82	72.22	72.01	70.54
S	1.53	1.62	1.52	1.58	1.42	1.45	1.54	1.91	1.83	1.64
Se	15.94	15.88	15.62	15.12	15.11	14.94	16.58	16.22	16.48	16.00
Te	7.31	7.75	8.29	8.47	9.06	9.64	7.50	5.88	5.78	7.89
total	100.16	100.31	99.47	100.36	101.14	101.72	100.41	100.77	100.71	100.30
Formulae (Σ S + Se + Te = 3)										
Pb	0.19	0.17	0.14	0.17	0.14	0.15	0.21	0.19	0.20	0.17
Sb	0.04	0.04	0.04	0.04	0.04	0.04	0.03	0.03	0.02	0.04
Bi	3.31	3.26	3.26	3.32	3.37	3.33	3.17	3.33	3.32	3.21
Σ cations	3.54	3.47	3.44	3.53	3.55	3.52	3.41	3.55	3.54	3.42
S	0.47	0.49	0.46	0.48	0.43	0.44	0.45	0.57	0.55	0.49
Se	1.97	1.93	1.91	1.87	1.87	1.83	1.99	1.98	2.01	1.93
Te	0.56	0.58	0.63	0.65	0.69	0.73	0.56	0.44	0.44	0.59

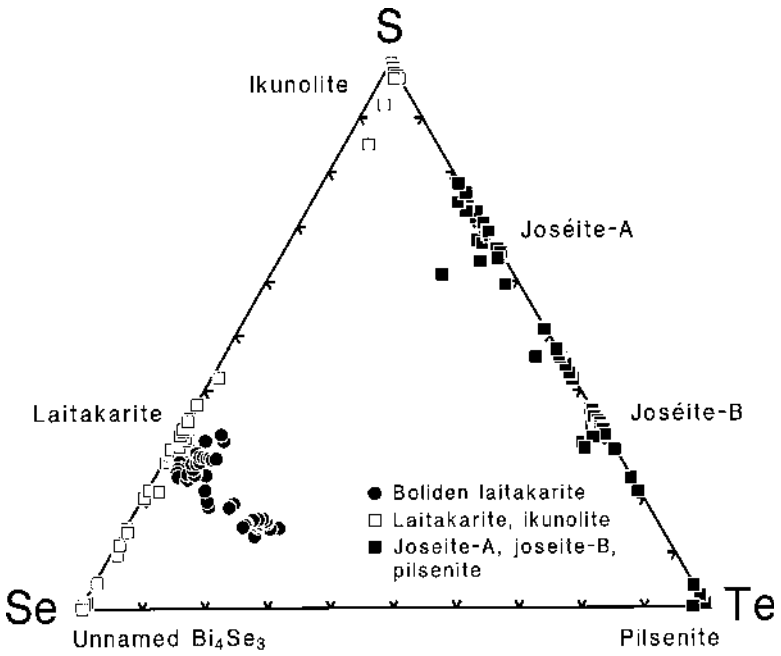

FIG. 6. Laitakarite compositions from the Boliden vein ores plotted in the system S–Se–Te. Analytical data on Bi sulfides, selenides and tellurides of the type $Bi_4(S,Se,Te)_3$ (laitakarite, ikunolite, joséite-A, joséite-B, pilsenite) reported in the literature are given for comparison (see text for references).

TABLE 6. REPRESENTATIVE RESULTS OF ELECTRON-MICROPROBE ANALYSES OF LAITAKARITE (PRODUCT OF DECOMPOSITION OF KOBELLITE), BOLIDEN MASSIVE SULFIDE DEPOSIT

	EJ-B3a 6	EJ-B3a 9	EJ-B3a 21	EJ-B3a 24	EJ-B3b 47	EJ-B6a 25	EJ-B6a 26	EJ-B6a 41	EJ-B6c 42	EJ-B8 55
Cu wt.%	0.26	0.13	<0.1	0.13	<0.1	<0.1	<0.1	<0.1	0.12	<0.1
Pb	3.21	3.75	3.60	3.10	3.46	3.46	3.27	3.33	3.35	3.68
Sb	0.13	0.34	0.34	0.33	0.26	0.44	0.50	0.19	0.15	0.29
Bi	75.67	72.87	74.62	76.44	73.70	74.28	75.00	76.01	75.21	74.70
S	2.80	1.93	2.42	3.11	2.43	2.45	2.40	2.49	2.39	2.30
Se	16.31	17.06	17.17	14.83	16.59	17.02	16.70	17.15	17.63	17.14
Te	1.71	4.08	1.94	2.53	3.16	2.30	2.24	1.05	1.33	2.10
total	100.09	100.16	100.09	100.47	99.60	99.95	100.11	100.22	100.18	100.21
	Formulae (Σ S + Se + Te = 3)									
Pb	0.15	0.18	0.17	0.15	0.16	0.16	0.16	0.16	0.16	0.17
Sb	0.01	0.03	0.03	0.03	0.02	0.03	0.04	0.02	0.01	0.02
Bi	3.53	3.39	3.47	3.60	3.41	3.44	3.54	3.60	3.50	3.51
Σ cations	3.69	3.60	3.67	3.78	3.59	3.63	3.74	3.78	3.67	3.70
S	0.85	0.59	0.74	0.95	0.73	0.74	0.74	0.77	0.73	0.70
Se	2.02	2.10	2.12	1.85	2.03	2.09	2.09	2.15	2.17	2.13
Te	0.13	0.31	0.15	0.20	0.24	0.17	0.17	0.08	0.10	0.16

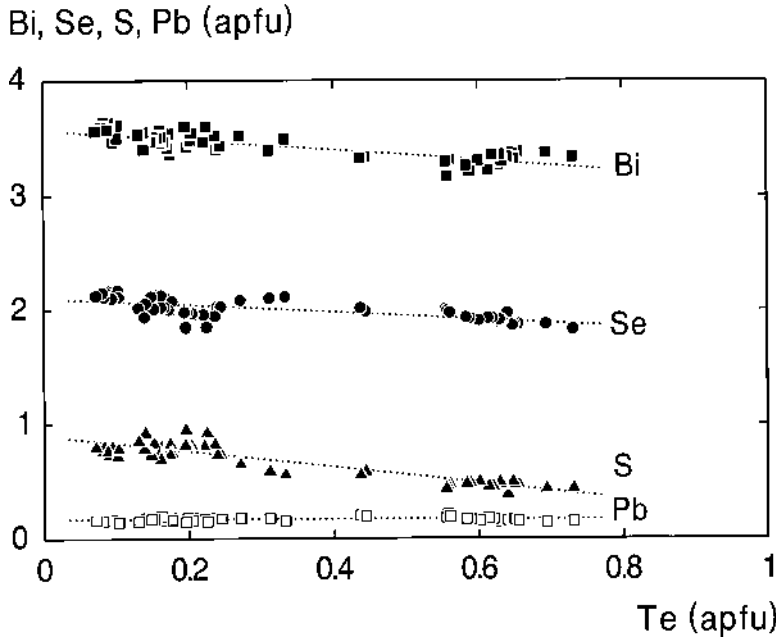

FIG. 7. Compositional range of laitakarite from the Boliden deposit. The numbers of Bi, Se, S and Pb *apfu* are plotted as a function of Te in *apfu*.

MODELS OF THE DECOMPOSITION REACTIONS

Textural relationships indicate that the observed assemblages that result from decomposition are related to interaction of the pre-existing vein ores with the fluid phase present. Therefore, modeling of the decomposition reactions requires the application of a method used for the quantification of metasomatic alteration. The calculation of balanced reactions has been performed for representative examples of the various textures using the isocon method (Grant 1986). Mean compositions of individual mineral phases were recalculated to a common basis of 70 S atoms; volume percentages of minerals within selected areas of the decomposition textures were determined by a VIDS V image-processing system. The volume data were corrected for density differences using literature data on cell dimensions and unit-cell volume. Details of the calculation procedure can be found in Ni Wen *et al.* (1991) and Wagner & Cook (1997). We estimate the error of the mass-balance calculations to be on the order of 10%, reflecting the relatively large uncertainty in the determination of volume proportions.

The reaction kobellite ⇒ selenian galena + laitakarite

Mean compositions (atomic concentration) of the individual mineral phases involved in this reaction as well as the bulk composition of the decomposition assemblage are given in Table 7a, whereas Table 7b contains the volume data. The cell dimensions of kobellite and laitakarite were taken from the JCPDS powder-diffraction file (datasets 73–1137 and 14–0220), whereas the cell dimension of selenian galena was derived from the relationship given by Liu & Chang (1994). The isocon diagram (Fig. 8) constructed for this decomposition reaction shows no ideal two-element isocon, although Bi and S are located relatively close to a straight line. On the basis of the assumption of relatively immobile behavior of both Bi and S, an influx of major amounts of Pb and Se can be assumed, whereas Sb, Cu and Fe have been removed. The reaction can be written as:

$$\begin{aligned} &Cu_{2.12}Fe_{1.83}Ag_{0.57}Pb_{21.29}(Sb_{18.35}Bi_{12.04})(S_{64.10}Se_{5.90}) \\ &+ 0.02\ Ag + 36.14\ Pb + 1.96\ Bi + 11.85\ Se \\ &+ 0.43\ Te \Rightarrow 59.22\ Ag_{0.01}Bi_{0.02}Pb_{0.96}(S_{0.66}Se_{0.34}) \\ &+ 3.59\ Pb_{0.16}Sb_{0.02}Bi_{3.57}(S_{0.76}Se_{2.12}Te_{0.12}) \\ &+ 2.12\ Cu + 1.83\ Fe + 18.28\ Sb + 22.29\ S \end{aligned} \quad (1)$$

Mobilization of elements from the gudmundite inclusions within kobellite, which are surrounded by the decomposition assemblage selenian galena + laitakarite, seems to have been of no importance to the reaction process. None of the elements (Fe, Sb, S) contained in gudmundite is enriched in one of the reaction products,

TABLE 7a. MEAN COMPOSITIONS (ATOMIC CONCENTRATION) OF PHASES INVOLVED INTO THE DECOMPOSITION REACTION KOBELLITE → SELENIAN GALENA + LAITAKARITE

	Kobellite $n = 15$	Galena $n = 10$	Laitakarite $n = 6$	Bulk int.
Cu at.%	1.68	0	0	0
Ag	0.45	0.53	0	0.45
Fe	1.45	0	0	0
Pb	16.87	48.21	2.30	41.14
Sb	14.54	0	0.36	0.06
Bi	9.54	0.84	52.90	9.86
S	50.79	33.35	11.28	29.95
Se	4.68	17.07	31.45	19.29
Te	0	0	1.71	0.26
total	100.0	100.0	100.0	100.01

The last column shows the composition of the bulk intergrowth (Bulk int.)

TABLE 7b. VOLUME DATA FOR THE DECOMPOSITION REACTION KOBELLITE → SELENIAN GALENA + LAITAKARITE

	Kobellite	Galena	Laitakarite
Vol.% in intergrowth		81.3	18.7
Volume per 70 S atoms (Å³)	3108.9	3798.9	4801.1
% in intergrowth on 70-S basis		84.6	15.4

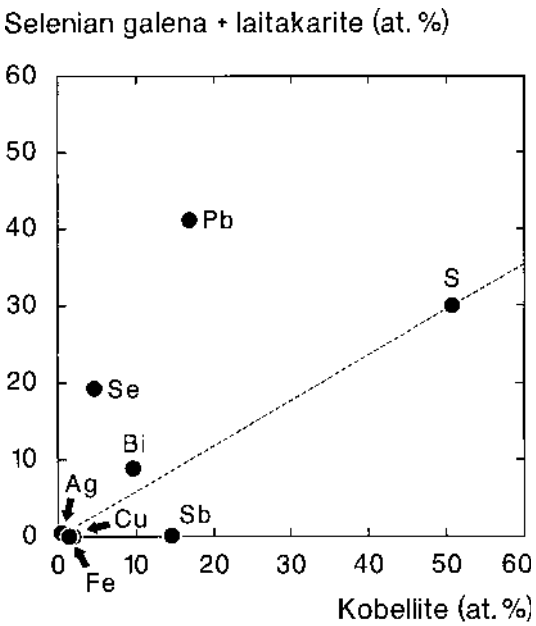

FIG. 8. Isocon diagram constructed for the decomposition reaction kobellite ⇒ selenian galena + laitakarite.

and corrosion of the gudmundite inclusions by the decomposition assemblage is relatively limited.

The reaction kobellite ⇒ tetrahedrite + laitakarite

Mean compositions and volume data are given in Tables 8a and 8b, respectively. For kobellite and laitakarite, the same unit-cell volume data as for reaction (1) were used, whereas the cell dimension of tetrahedrite was calculated using the equation of Johnson *et al.* (1986). The isocon diagram (Fig. 9) suggests a relative immobility of both Sb and S and a net change in mass close to unity. A significant supply of several elements with a high diffusivity, including Cu, Fe, Ag and Zn, can be deduced from the isocon diagram, whereas Pb, Bi and Se have been removed during the decomposition reaction. The reaction can thus be written as:

$$Cu_{2.65}Fe_{1.50}Ag_{0.49}Pb_{21.46}(Sb_{18.48}Bi_{11.73})(S_{64.11}Se_{5.89}) + 41.27\ Cu + 6.68\ Fe + 1.49\ Zn + 4.42\ Ag + 1.43\ Sb + 1.01\ S + 0.20\ Te \Rightarrow 4.96\ (Cu_{8.83}Ag_{0.99})(Fe_{1.65}Zn_{0.30})(Sb_{4.01}Bi_{0.02})(S_{12.96}Se_{0.04}) + 1.13\ Cu_{0.11}Pb_{0.19}Sb_{0.02}Bi_{3.36}(S_{0.74}Se_{2.08}Te_{0.18}) + 21.24\ Pb + 7.83\ Bi + 3.34\ Se \quad (2)$$

Most of the Cu and Fe concentrated in tetrahedrite formed by this reaction can be derived from chalcopyrite, which is still present as corroded relict grains within

TABLE 8a. MEAN COMPOSITIONS (ATOMIC CONCENTRATION) OF PHASES INVOLVED INTO THE DECOMPOSITION REACTION KOBELLITE → TETRAHEDRITE + LAITAKARITE

	Kobellite $n = 8$	Tetrahedrite $n = 8$	Laitakarite $n = 1$	Bulk int.
Cu at.%	2.10	30.68	1.67	29.23
Ag	0.39	3.42	0	3.25
Fe	1.18	5.73	0	5.44
Zn	0	1.05	0	1.00
Pb	16.99	0	2.78	0.14
Sb	14.63	13.91	0.26	13.23
Bi	9.29	0.06	50.35	2.58
S	50.76	45.01	11.10	43.32
Se	4.66	0.13	31.22	1.69
Te	0	0	2.62	0.13
total	100.0	99.99	100.0	100.01

The last column shows the composition of the bulk intergrowth (Bulk int.).

TABLE 8b. VOLUME DATA FOR THE DECOMPOSITION REACTION KOBELLITE → TETRAHEDRITE + LAITAKARITE

	Kobellite	Tetrahedrite	Laitakarite
Vol.% in intergrowth		92.4	7.6
Volume per 70 S atoms (Å³)	3108.9	3068.0	4801.1
% in intergrowth on 70-S basis		95.0	5.7

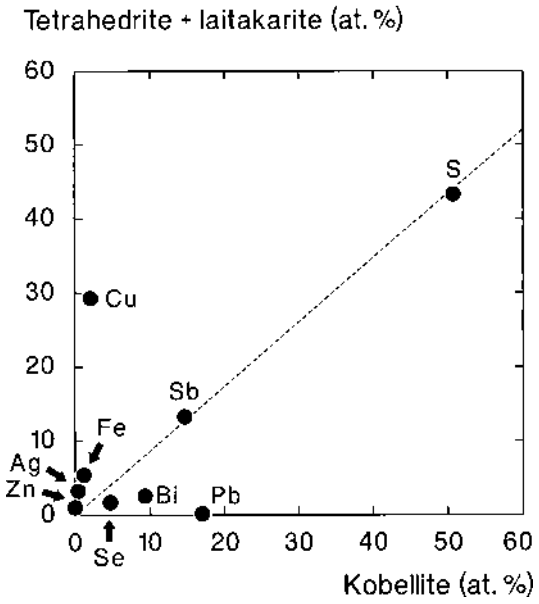

FIG. 9. Isocon diagram for the decomposition reaction kobellite ⇒ tetrahedrite + laitakarite.

the decomposition assemblage. In contrast, Ag and Zn must have been supplied by the fluids involved in the reaction, because no precursor mineral containing these elements has been found in proximity of the tetrahedrite–laitakarite intergrowths.

The reaction kobellite ⇒ bournonite + laitakarite

Mean compositions and volume data are given in Tables 9a and 9b, respectively. The cell dimensions of kobellite, bournonite and laitakarite were derived from the JCPDS powder-diffraction data file (datasets 73–1137, 42–1406 and 14–0220). The isocon diagram constructed for this decomposition reaction indicates a relatively immobile behavior of Pb and S, although Sb is also located very close to the straight line defined by Pb and S (Fig. 10). Removal of Bi, Fe and Ag is suggested, whereas significant amounts of Cu must have been added during the reaction. The reaction can be written as:

$$Cu_{2.49}Fe_{1.61}Ag_{0.48}Pb_{21.38}(Sb_{18.31}Bi_{12.22})(S_{64.16}Se_{5.84}) + 19.40\ Cu + 0.19\ Pb + 2.84\ Sb + 2.67\ Se + 0.24\ Te \Rightarrow 21.78\ Cu_{1.00}Pb_{0.98}(Sb_{0.97}Bi_{0.04})(S_{2.73}Se_{0.27}) + 1.32\ Cu_{0.08}Pb_{0.17}Sb_{0.02}Bi_{3.48}(S_{0.83}Se_{1.99}Te_{0.18}) + 1.61\ Fe + 0.48\ Ag + 6.75\ Bi + 3.60\ S \quad (3)$$

TABLE 9a. MEAN COMPOSITIONS (ATOMIC CONCENTRATION) OF PHASES INVOLVED INTO THE DECOMPOSITION REACTION KOBELLITE = BOURNONITE + LAITAKARITE

	Kobellite $n=7$	Bournonite $n=6$	Laitakarite $n=8$	Bulk int.
Cu at.%	1.97	16.76	1.15	15.87
Ag	0.38	0	0	0
Fe	1.27	0	0	0
Pb	16.90	16.27	2.50	15.49
Sb	14.47	16.20	0.29	15.29
Bi	9.66	0.71	51.56	3.61
S	50.72	45.60	12.25	43.70
Se	4.62	4.46	29.56	5.89
Te	0	0	2.69	0.15
total	99.99	100.00	100.00	100.00

The last column shows the composition of the bulk intergrowth (Bulk int.).

TABLE 9b. VOLUME DATA FOR THE DECOMPOSITION REACTION KOBELLITE = BOURNONITE + LAITAKARITE

	Kobellite	Bournonite	Laitakarite
Vol.% in intergrowth		91.8	8.2
Volume per 70 S atoms (Å^3)	3108.9	3227.2	4801.1
% in intergrowth on 70-S basis		94.3	5.7

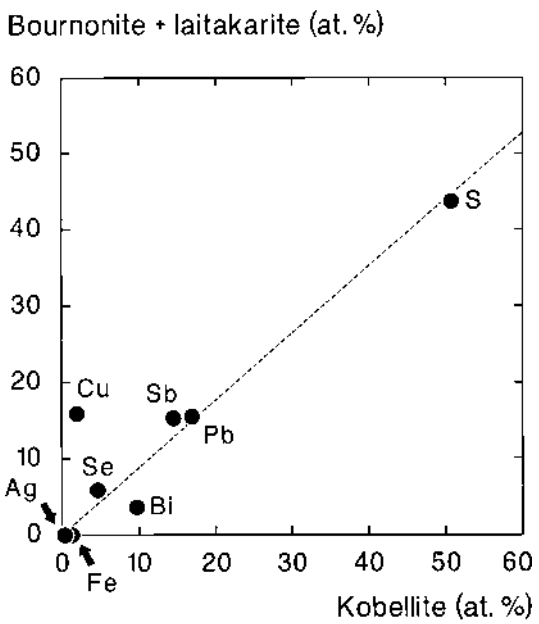

FIG. 10. Isocon diagram for the decomposition reaction kobellite ⇒ bournonite + laitakarite.

Although the decomposition of kobellite to a bournonite–laitakarite intergrowth is clearly restricted to grain boundaries between kobellite and arsenopyrite, significant mobilization of elements from arsenopyrite (Fe, As, S) and fixation within the decomposition assemblage have not been detected. On the basis of mass-balance calculations, it is obvious that the various decomposition-reactions discussed above do not represent a simple breakdown of kobellite, but they relate to complex fluid-assisted diffusion-controlled processes accompanied by addition and removal of components.

Discussion

Composition of minerals of the joséite subgroup

Tellurian laitakarite comparable in composition to the Boliden examples has not been reported to date. A meaningful interpretation of these Te-rich compositions of laitakarite requires an extensive compilation and discussion of the available literature on Bi sulfotelluride and sulfoselenide compositions. The known phases in the pseudoternary system Bi_4S_3 – Bi_4Se_3 – Bi_4Te_3 belonging to the joséite subgroup of the tetradymite group include the following naturally occurring species: ikunolite, Bi_4S_3, joséite-A, Bi_4S_2Te, joséite-B, Bi_4Te_2S, pilsenite, Bi_4Te_3, laitakarite, $Bi_4(Se,S)_3$ (Kato 1959, Vorma 1960, Ozawa & Shimazaki 1982, Bayliss 1991) and an unnamed Cu-bearing Bi_4Se_3 phase described by Piestrzynski (1992). On the basis of investigations of crystal structure, which indicate the absence of Te and S order in Bi sulfotelluride phases belonging to the space group *R*3*m* (including minerals of the tetradymite and joséite subgroups), a complete solid-solution series between pilsenite and ikunolite has been proposed (Bayliss 1991). However, reported compositions of sulfotellurides along the Bi_4S_3–Bi_4Te_3 join (Zavyalov & Begizov 1978, Bortnikov *et al.* 1982, Bonev 1986, Dobbe 1993, Simon & Alderton 1995) indicate that pilsenite and the intermediate phases joséite-A and joséite-B possess relatively fixed stoichiometries (Fig. 6). A limited number of micro-analytical data, which plot between the ideal compositions of ikunolite, joséite-A, joséite-B and pilsenite (Mintser *et al.* 1968, Godovikov *et al.* 1970, Zavyalov & Begizov 1983, Yingchen 1986, Kato *et al.* 1994), indicate that such a solid-solution relationship is indeed found in nature. The isostructural relationship between laitakarite and ikunolite, which both possess the space group *R*3*m*, should make an extensive solid-solution along the Bi_4S_3–Bi_4Se_3 join possible. In contrast to this, solid solution between laitakarite and ikunolite (Bi_4S_3) seems to be relatively limited, and most compositions of ikunolite are located very close to the Bi_4S_3 end-member (Nechelyustov *et al.* 1978, Finashin *et al.* 1979, Bortnikov *et al.* 1982, Imai & Chung 1986). Most of the laitakarite compositions reported in the literature display a Se:S ratio very close to 2:1, but a relatively limited number of compositions are richer in Se (Kovalenker & Geynke 1984, Yushko *et al.* 1984), including an unnamed phase corresponding to the S-free Bi_4Se_3 end-member, which has been described from Kupferschiefer-type mineralization (Piestrzynski 1992). Two compositions of joséite-A and joséite-B reported by Bortnikov *et al.* (1982) indicate that limited but nevertheless substantial incorporation of Se into Bi sulfotelluride phases may be possible.

Additional complications affecting the interpretation of natural compositions in the system Bi_4S_3–Bi_4Se_3–Bi_4Te_3 arise from the presence of intimate intergrowths involving some of these mineral phases (*e.g.*, Markham 1962, Zavyalov & Begizov 1978). However, the array of compositional data suggests that the Te-rich laitakarite phase from the Boliden vein ores cannot be explained by a physical mixture of laitakarite and one of the Bi sulfotellurides. The compositions of Te-rich laitakarite in S–Se–Te space are not located on a linear trend connecting laitakarite with either joséite-A, joséite-B or pilsenite (Fig. 6). Such a linear trend would be expected for analytical data related to variable mixtures of two more-or-less stoichiometric phases. In addition, back-scattered electron imaging of several Te-rich lath-shaped crystals of laitakarite has shown that neither inhomogeneity nor compositional zonation is present. Therefore, we conclude that the tellurian laitakarite from the Boliden deposit represents a true ternary phase in the system Bi_4S_3–Bi_4Se_3–Bi_4Te_3, indicative of extensive solid-solution relationships among the Bi sulfotellurides and sulfoselenides.

The analytical data for laitakarite from the Boliden vein ores demonstrate that Pb constitutes an essential component. This is consistent with most compositions of laitakarite and ikunolite reported in the literature, which show a similar range of Pb incorporation (2.92–5.80 wt.% Pb). The only exception is represented by four datasets reported by Kovalenker & Geynke (1984), which contain a relatively low but still detectable concentration of Pb (0.13–0.60 wt.%). In contrast, the Bi sulfotellurides (joséite-A, joséite-B, pilsenite) and the unnamed Bi_4Se_3 phase (Piestrzynski 1992) are essentially Pb-free or contain much lower concentrations of Pb, in the range 0.2–1.34 wt.% (Zavyalov & Begizov 1978, Bortnikov *et al.* 1982, Bonev 1986, Dobbe 1993). Compared to other Pb-bearing Bi selenide and telluride phases, like rucklidgeite ($PbBi_2Te_4$), aleksite ($PbBi_2Te_2S_2$) and poubaite ($PbBi_2Te_2Se_2$), which possess a relatively stoichiometric amount of Pb incorporated in the structure (Johan *et al.* 1987), the composition of Bi sulfoselenides of the laitakarite–ikunolite group seems to be more variable.

Laitakarite from the Boliden vein-type ores displays a significant deficiency in cations, when normalized to (S + Se + Te) = 3 *apfu*. This finding is consistent with a large number of published compositions of laitakarite, whereas the reported composition of ikunolite, joséite-A and joséite-B tend to be closer to the ideal stoichiometry. The observed negative correlation between Bi and

Te and the deficiency in cations may be explained by a partial substitution of Te^{4+} for Bi^{3+} on the cation sites (Zavyalov & Begizov 1983). A similar mechanism has been invoked for the observed trends of substitution in Te-rich tetrahedrite (Makovicky 1989). If part of the Te incorporated into laitakarite occupies cation sites, this would result in a better overall stoichiometry. Substitution of Te^{4+} for Bi^{3+} results in an excess in the number of positive charges, which would require a compensation by vacancies at the *B* site.

Genetic considerations

The results of our study demonstrate that the mineral assemblages in the vein ore from Boliden are the result of a complex mineralogical and textural evolution. Comparison of the sulfide–sulfosalt associations with experimental data on sulfide phase equilibria can be used to place some constraints on the late-stage evolution of the Boliden deposit. A rigorous discussion would require information on phase equilibria in the multi-element system Cu–Fe–Ag–Pb–Sb–Bi–S–Se–Te, but available experimental data are restricted to less complex subsystems of this system.

Synthetic equivalents of kobellite and tintinaite have been found in experimental studies of the systems PbS–Sb_2S_3–Bi_2S_3 (Chang *et al.* 1980), FeS–PbS–Sb_2S_3–Bi_2S_3 (Chang *et al.* 1980) and Cu_2S–PbS–Sb_2S_3 (Pruseth *et al.* 1997, 1998). Fe-free and Fe-rich kobellite form a complete solid-solution series at temperatures of 500 and 450°C, whereas at 400°C, both phases were found no longer to be stable. The decomposition of kobellite occurs at a temperature of about 430°C (Chang *et al.* 1980). Experimental studies of the system Cu_2S–PbS–Sb_2S_3 have shown that a synthetic analogue of tintinaite is stable at temperatures around 440°C, whereas at 300°C this phase is not stable (Pruseth *et al.* 1997, 1998). Interestingly, the compositional limits of synthetic kobellite-type phases coincide well with data on solid solution involving Bi–Sb in natural kobellite. Natural tintinaite–kobellite samples are characterized by a complete range of solid solution between the Sb end-member and a composition with a Bi/(Bi + Sb) value close to 0.65–0.68 (Moëlo *et al.* 1995), which apparently is the compositional limit obtained in experimental studies. In conclusion, the stability of the tintinaite–kobellite solid-solution series seems to be confined to a relatively limited interval of temperature of about 350–450°C, which can also be assumed as a reasonable estimate for the formation of kobellite in the Boliden vein ores.

The observed destabilization of kobellite and the composition of selenian galena indicate that temperatures of formation were significantly lower during the post-deformational evolution of the vein ores. The range of Te incorporation into selenian galena having a S:Se ratio of approximately 2:1 is restricted to about 5 mol.% at a temperature of 300°C (Liu & Chang 1994). Selenian galena formed at the expense of kobellite has a composition close to $Pb_{1.00}(S_{0.67}Se_{0.33})$ and contains very low concentrations of Te, <0.2 wt.%. These compositional characteristics are in agreement with temperatures below 300°C. Unfortunately, the presence of laitakarite in all decomposition assemblages cannot be used to estimate the temperatures of formation. According to the limited experimental data on phase equilibria in the systems Bi–Se–S and Bi–Te–S, laitakarite is stable in the temperature range between 100 and 470°C (Afifi *et al.* 1988, Simon & Essene 1996).

In a microthermometric study of the Boliden vein assemblages, Åberg (1995) suggested that the quartz within the arsenopyrite-hosted veins formed at a minimum temperature of around 200°C. Considering that no pressure correction was applied, a significantly increased temperature would fit the stability limits estimated for the sulfide–sulfosalt minerals fairly well. A correction of fluid-inclusion temperature data for pressure seems needed in view of the microthermometric data presented by Broman (1992), indicating pressures of 2.2 ± 0.5 kbar for the Boliden quartz-bearing vein assemblages. According to Bergman Weihed *et al.* (1996), brecciation of the arsenopyrite ore and subsequent formation of the assemblage quartz – sulfosalt – sulfide – gold, as well as the deformation of the veins, occurred prior to the regional peak metamorphism, the latter event resulting in the observed recrystallization of the arsenopyrite. If this interpretation is correct, the temperature estimates for the vein-hosted sulfide–sulfosalt association presented in this study also place some constraints on the regional metamorphism of this part of the Skellefte district. In a study that applied arsenopyrite geothermometry and sphalerite geobarometry, Berglund & Ekström (1978) suggested that peak conditions of metamorphism in the Boliden area attained 430°C and 5–7 kbar. These temperatures coincide well with our temperature estimates for kobellite and would suggest an initial formation of the sulfosalt-rich vein assemblages close to peak conditions of metamorphism.

The patterns of element mobility or immobility derived for the three types of decomposition reactions do not point to interaction of the sulfosalt-rich vein ores with an externally derived fluid phase during this late stage of vein evolution. We cannot recognize any general pattern of enrichment or depletion of specific elements that could be related to the introduction of an external fluid and that could result in similar reaction-pathways for the decomposition reactions involving kobellite. It seems more likely that these reactions are related to a stage of internal equilibration of the vein assemblages, dominantly controlled by local mobilization and redistribution of elements with a relatively high diffusivity such as Cu, Ag, Fe and Zn. The decomposition reactions were most probably controlled by chemical potential gradients within the veins, which evolved during the post-deformation retrograde P–T evolution of the Boliden deposit.

Conclusions

(1) Vein-type mineralization from the Boliden massive sulfide deposit, hosted by brecciated arsenopyrite, carries a complex assemblage of ore minerals, including several Se-rich sulfosalt and selenide phases. Selenian kobellite is the dominant sulfosalt mineral present.

(2) Three distinct types of decomposition assemblages, which postdate the deformation of the vein ores, have formed at the expense of kobellite. These are (i) selenian galena + laitakarite, (ii) tetrahedrite + laitakarite, and (iii) bournonite + laitakarite.

(3) Laitakarite displays a broad compositional variability. Substantial Te incorporation into laitakarite, in the range of 0.94–9.64 wt.% and not reported previously, has implications for solid-solution relationships among Bi phases of the joséite subgroup. The observed ternary compositions in the system Bi_4S_3–Bi_4Se_3–Bi_4Te_3 are in accordance with crystal-chemical predictions.

(4) Pb in the concentration range 3.01–4.56 wt.% constitutes an essential component of laitakarite from Boliden. The Pb concentration is approximately constant over the entire compositional range, including both Te-rich and Te-poor varieties.

(5) Thermal constraints on the kobellite-rich sulfosalt assemblage suggest temperatures in the range 350–450°C for their formation, which narrows previously inferred conditions of formation.

Acknowledgements

We thank P. Spaethe for preparation of polished sections, and K.P. Kelber for the black and white photographs. We thank A. Henk (Institute of Geology, University of Würzburg) for his introduction to the use of the VIDS V image-processing system. We thank two anonymous referees, Associate Editor F. Vurro, and Robert F. Martin for their helpful comments, which have significantly improved this paper.

References

Åberg, A. (1995): Fluid evolution in the gold lode ores at Boliden; a key to metallogenesis in the Boliden deposit. *Swedish National Board for Industrial and Technical Development, Report of the National Ore Geology Research Programme* **93-0135P**.

Afifi, A.M., Kelly, W.C. & Essene, E.J. (1988): Phase relations among tellurides, sulfides, and oxides. I. Thermochemical data and calculated equilibria. *Econ. Geol.* **83**, 377-394.

Allen, R.L., Weihed, P. & Svenson, S.Å. (1996): Setting of Zn–Cu–Au–Ag massive sulfide deposits in the evolution and facies architecture of a 1.9 Ga marine volcanic arc, Skellefte district, Sweden. *Econ. Geol.* **91**, 1022-1053.

Bayliss, P. (1991): Crystal chemistry and crystallography of some minerals in the tetradymite group. *Am. Mineral.* **76**, 257-265.

Berglund, S. & Ekström, T.K. (1978): Arsenopyrite and sphalerite as T–P indicators in sulfide ores from northern Sweden. *Mineral. Deposita* **15**, 175-187.

Bergman Weihed, J., Bergström, U., Billström, K. & Weihed, P. (1996): Geology, tectonic setting, and origin of the Paleoproterozoic Boliden Au–Cu–As deposit, Skellefte district, northern Sweden. *Econ. Geol.* **91**, 1073-1097.

Billström, K. & Weihed, P. (1996): Age and provenance of host rocks and ores in the Paeoproterozoic Skellefte district, northern Sweden. *Econ. Geol.* **91**, 1054-1072.

Bonev, I.I. (1986): Betekhtinite and joséite-B from the Propada deposit, Malko Tirnovo–Bourgas district. *Dokl. Bolgarskoy Akad. Nauk* **39**, 59-62 (in Bulg.).

Bortnikov, N.S., Mozgova, N.N., Nekrasov, I.Y., Rozov, D.N., Tupyakov, V.Y. & Tsepin, A.I. (1982): Particularities of bismuth mineralization in gold ores of eastern Transbaikalia. *Mineral. Zh.* **4**, 45-58 (in Russ.).

Broman, C. (1992): Origin of massive sulfide ores in the Skellefte district, as indicated by fluid inclusions. *Medd. Stockh. Univ. Inst. Geol. Geokem.* **286**.

Chang, L.L.Y., Walia, D.S. & Knowles, C. (1980): Phase relations in the system PbS–Sb_2S_3–Bi_2S_3 and PbS–FeS–Sb_2S_3–Bi_2S_3. *Econ. Geol.* **75**, 317-328.

Cook, N.J. (1997): Bismuth and bismuth–antimony sulphosalts from Neogene vein mineralisation, Baia Borsa area, Maramures, Romania. *Mineral. Mag.* **61**, 387-409.

Dobbe, R. (1993): Bismuth tellurides (joséite-B, bismuthian tsumoite) in a Pb–Zn deposit from Tunaberg, Sweden. *Eur. J. Mineral.* **5**, 165-170.

Finashin, V.K., Litavrina, R.F., Romanenko, I.M. & Chubarov, V.M. (1979): Ikunolite from the Vysokogora deposit, Primorye. *Zap. Vses. Mineral. Obshchest.* **108**, 337-339 (in Russ.).

Foord, E.E. & Shawe, D.R. (1989): The Pb–Bi–Ag–Cu–(Hg) chemistry of galena and some associated sulfosalts: a review and some new data from Colorado, California and Pennsylvania. *Can. Mineral.* **27**, 363-382.

Godovikov, A.A., Kochetkova, K.V. & Bogdanova, V.I. (1970): Study of the bismuth sulfotellurides of the Sokhondo deposit. *Geol. Geofiz.* **11**, 123-127 (in Russ.).

Grant, J.A. (1986): The isocon diagram – a simple solution to Gresen's equation for metasomatic alteration. *Econ. Geol.* **81**, 1976-1982.

Grip, E. & Wirstam, Å. (1970): The Boliden sulphide deposit. A review of geo-investigations carried out during the lifetime of the Boliden mine, Sweden (1924–1967). *Sver. Geol. Unders.* **C 651**.

HARRIS, D.C., JAMBOR, J.L., LACHANCE, G.R. & THORPE, R.I. (1968): Tintinaite, the antimony analogue of kobellite. *Can. Mineral.* **9**, 371-382.

IMAI, N. & CHUNG, J.I. (1986): The first Korean occurrence of ikunolite. *Mineral. J.* **13**, 65-74.

ISAKSSON, I. (1973): Vismut–antimonrika mineraliseringar i Bolidenmalmen. Licentiate thesis, Univ. of Stockholm, Stockholm, Sweden (in Swedish).

JOHAN, Z., PICOT, P. & RUHLMANN, F. (1987): The ore mineralogy of the Otish Mountains uranium deposit, Quebec: skippenite, Bi_2Se_2Te, and watkinsonite, $Cu_2PbBi_4(Se,S)_8$, two new mineral species. *Can. Mineral.* **25**, 625-638.

JOHNSON, N.E., CRAIG, J.R. & RIMSTIDT, J.D. (1986): Compositional trends in tetrahedrite. *Can. Mineral.* **24**, 385-397.

KARUP-MØLLER, S. (1970): Weibullite, laitakarite, and bismuthinite from Falun, Sweden. *Geol. Fören. Stockholm Förh.* **92**, 181-187.

KATO, A. (1959): Ikunolite, a new bismuth mineral from the Ikuno mine, Japan. *Mineral J.* **2**, 397-407.

_____, SHIMIZU, M., SUZUKI, Y., OKADA, Y. & KOMURO, Y. (1994): Joséite-A from Nagakuki, Hanawacho, Fukushima Prefecture, Japan. *Bull. Nat. Mus. Tokyo* **C 20**, 141-147.

KOVALENKER, V.A. & GEYNKE, V.R. (1984): A new type of Cu–Sn–Bi–Se mineralization in the Kuraminsk area of the middle Tien Shan. *Int. Geol. Rev.* **26**, 1093-1106.

LIU, H. & CHANG, L.L.Y. (1994): Phase relations in the system PbS–PbSe–PbTe. *Mineral. Mag.* **58**, 567-578.

MAKOVICKY, E. (1977): Chemistry and crystallography of the lillianite homologous series. III. Crystal chemistry of lillianite homologues. Related phases. *Neues Jahrb. Mineral., Abh.* **131**, 187-207.

_____ (1989): Modular classification of sulfosalts: current status. Definition and application of homologous series. *Neues Jahrb. Mineral., Abh.* **160**, 269-297.

_____ & MUMME, W.G. (1986): The crystal structure of izoklakeite, $Pb_{51.3}Sb_{20.4}Bi_{19.5}Ag_{1.2}Cu_{2.9}Fe_{0.7}S_{114}$: the kobellite homologous series and its derivatives. *Neues Jahrb. Mineral., Abh.* **153**, 121-145.

MARKHAM, N.L. (1962): Plumbian ikunolite from Kingsgate, New South Wales. *Am. Mineral.* **47**, 1431-1434.

MARSHALL, B. & GILLIGAN, L.B. (1989): Durchbewegung structure, piercement cusps, and piercement veins in massive sulfide deposits: formation and interpretation. *Econ. Geol.* **84**, 2311-2319.

MINTSER, E.F., MYMRIN, V.A. & ISAYEVA, K.G. (1968): Joséite A from central Asia. *Dokl. Acad. Sci. USSR, Earth Sci. Sect.* **178**, 114-117.

MOËLO, Y., JAMBOR, J.L. & HARRIS, D.C. (1984): Tintinaïte et sulfosels associés de Tintina (Yukon): la cristallochimie de la série de la kobellite. *Can. Mineral.* **22**, 219-226.

_____, ROGER, G., MAUREL-PALACIN, D., MARCOUX, E. & LAROUSSI, A. (1995): Chemistry of some Pb–(Cu, Fe)–(Sb, Bi) sulfosalts from France and Portugal. Implications for the crystal chemistry of lead sulfosalts in the Cu-poor part of the Pb_2S_2–Cu_2S–Sb_2S_3–Bi_2S_3 system. *Mineral. Petrol.* **53**, 229-250.

MÖRTSELL, S. (1931): Gediget guld i Boliden-malmen. *Geol. Fören. Stockholm Förh.* **53**, 394-414 (in Swedish).

NECHELYUSTOV, G.N., STEPANOV, V.I., SHUMKOVA, N.G. & KHALEZOVA, Y.B. (1978): Ikunolite, Bi_4S_3, from the Kara–Obo tungsten deposit, central Kazakhstan; the first discovery in the USSR. *Novye Dannye o Mineralah SSSR* **26**, 105-111 (in Russ.).

NENASHEVA, S.N., MOZGOVA, N.N., BORODAYEV, Y.S., YEFIMOV, A.V. & ORGANOVA, N.I. (1988): Relationship between the chemical composition and crystalline structure of laitakarite. *Dokl. Akad. Nauk SSSR* **303**, 1468-1472 (in Russ.).

NI WEN, ASHWORTH, J.R. & IXER, R.A. (1991): Evidence for the mechanism of the reaction producing a bournonite–galena symplectite from meneghinite. *Mineral. Mag.* **55**, 153-158.

ÖDMAN, O.H. (1938): On the mineral associations of the Boliden ore. *Geol. Fören. Stockholm Förh.* **413**, 121-146.

_____ (1941): Geology and ores of the Boliden deposit, Sweden. *Sver. Geol. Unders.* **C 438**.

OZAWA, T. & SHIMAZAKI, H. (1982): Pilsenite redefined and wehrlite discredited. *Proc. Japan Acad.* **58**, 291-294.

PIESTRZYNSKI, A. (1992): Bi_4Se_3, a new unnamed mineral from the Kuperschiefer, Polish Lowland; preliminary report. *Mineral. Polonica* **23**, 35-42.

PRUSETH, K.L., MISHRA, B. & BERNHARDT, H.J. (1997): Phase relations in the Cu_2S–PbS–Sb_2S_3 system: an experimental appraisal and application to natural polymetallic sulfide ores. *Econ. Geol.* **92**, 720-732.

_____, _____ & _____ (1998): Solid solution in synthetic zinkenite, robinsonite and meneghinite in the system Cu_2S–PbS–Sb_2S_3. *Can. Mineral.* **36**, 207-213.

RICKARD, D.T. (1986): The Skellefte field. *Sver. Geol. Unders.* **Ca 62**.

_____ & ZWEIFEL, H. (1975): Genesis of Precambrian sulfide ores, Skellefte district, Sweden. *Econ. Geol.* **70**, 255-274.

SIMON, G. & ALDERTON, D.H.M. (1995): Pilsenite, Bi_4Te_3, from the Sacaramb gold–telluride deposit, Metaliferi Mts; first occurrence in Romania. *Rom. J. Mineral.* **76**, 111-113.

_____ & ESSENE, E.J. (1996): Phase relations among selenides, sulfides, tellurides, and oxides. I. Thermodynamic properties and calculated equilibria. *Econ. Geol.* **91**, 1183-1208.

VIVALLO, W. (1987): Early Proterozoic bimodal volcanism, hydrothermal activity, and massive sulfide deposition in the Boliden-Långdal area, Skellefte District, Sweden. *Econ. Geol.* **82**, 440-456.

VORMA, A. (1960): Laitakarite, a new Bi–Se mineral. *Bull. Comm. Géol. Finlande* **188**, 1-10.

WAGNER, T. & COOK, N.J. (1997): Mineral reactions in sulphide systems as indicators of evolving fluid geochemistry – a case study from the Apollo mine, Siegerland, FRG. *Mineral. Mag.* **61**, 573-590.

WEIHED, P., BERGMAN, J. & BERGSTRÖM, U. (1992): Metallogeny and tectonic evolution of the Early Proterozoic Skellefte district, northern Sweden. *Precamb. Res.* **58**, 143-167.

YEFIMOV, A.V., NENASHEVA, S.N., BORODAYEV, Y.S., MOZGOVA, N.N. & SIVTSOV, A.V. (1988): Hypogene selenium mineralization on the Nevskoye tin ore deposit, northeastern USSR. *Novye Dannye o Mineralah SSSR* **35**, 128-151 (in Russ.).

YINGCHEN, REN (1986): Tellurobismuthinides from Pangushan, China. *Geochemistry* (*China*) **5**, 277-279.

YUSHKO, Z.O.Y., DUBAKINA, L.S., SHCHERBACHEV, D.K., STEPANOV, V.I. & BONDAREV, V.P. (1984): Bismuth selenides from the Vozhma Massif. *Dokl. Akad. Nauk SSSR* **275**, 729-732 (in Russ.).

ZAKRZEWSKI, M.A. & MAKOVICKY, E. (1986): Izoklakeite from Vena, Sweden, and the kobellite homologous series. *Can. Mineral.* **24**, 7-18.

ZAVYALOV, Y.N. & BEGIZOV, V.D. (1978): New types of bismuth sulfotellurides. *Izv. Vysshikh Uchebnykh Zavedeniy, Geologiya i Razvedka* **10**, 91-100 (in Russ.).

_____ & _____ (1983): New data on the constitution and nomenclature of the sulfotellurides of bismuth of the joséite group. *Zap. Vses. Mineral. Obshchest.* **112**, 589-601 (in Russ.).

_____, _____ & CHVILEVA, T.N. (1983): New data on laitakarite. *Zap. Vses. Mineral. Obshchest.* **117**, 185-192 (in Russ.).

Received July 17, 2000, revised manuscript accepted May 8, 2001.